Advances and Applications in Mathematical Sciences
Volume 23, Issue 5, March 2024, Pages 389-403

COMBINED EFFECTS OF SORET AND DUFOUR ON MHD FLOW THROUGH POROUS MEDIUM PAST AN INCLINED CYLINDER WITH VARIABLE OSCILLATING WALL TEMPERATURE AND MASS DIFFUSION

MANISH KUMAR[1], GAURAV KUMAR[2] and ABDUL WADOOD KHAN[3]

[1,3]Department of Mathematics and statistic
Integral University, Lucknow, India
E-mail: mkumarmath84@gmail.com
awkhan@iul.ac.in

[2]Department of Mathematics and Computer Science
BBD University, Lucknow, U.P, India
E-mail: logontogauravsharma@gmail.com

Abstract

The present study is carried out to examine the combined effects of Soret and Dufour on unsteady flow of a viscous, incompressible and electrically conducting fluid past through inclined cylinder in the presence of transversely applied uniform magnetic field. In the Fluid model, the medium of the fluid flow has been taken porous and the geometry of cylinder is inclined at an angle ϕ from vertical plane. The temperature of the fluid near the surface of cylinder is oscillating and concentration level near the surface increase linearly with time. The non-dimensional governing equations have been solved numerically by using Crank-Nicolson implicit finite difference method and also discussed the stability of the solution. The velocity profile is discussed with the help of graphs drawn for different parameters and the solution of the MHD flow model is unconditionally stable. Therefore, the scheme is compatible. Stability and compatibility ensures convergence.

1. Introduction

The effects of chemical reaction on free convection boundary layer over a various shapes such as plate, sphere and others have been studied among researchers because it has become more important recently. The chemical

2020 Mathematics Subject Classification: 76W05, 76D05, 80A20.
Keywords: MHD flow, Soret effect, Dufour effect, porous medium.
Received September 29, 2023; Accepted October 17, 2023

reaction effect along with influence of magnetic field on such a flow within porous media has play important role in engineering applications. Heat transfer analysis of boundary layer flow over hyperbolic stretching cylinder was studied by Majeed et al. [1] and they have obtained the numerical results for the model by using Keller box method. They noticed that, increase in the values of curvature parameter leads to increase in velocity and temperature distribution. They have also found the skin-friction coefficient reduces and Nusselt number enhances with an increase in curvature parameter. Soret and Dufour effects on mixed convection along a vertical wavy surface in a porous medium with variable properties were explained by Srinivasacharya et al. [2]. In their paper, the governing flow model solved numerically and explained the flow velocity and concentration of fluid are decreased with increases in Dufour number while the temperature and rate of heat and mass transfer are enhanced consistently. Kumar et al. [3] worked on chemical reaction effect on MHD flow past an impulsively started vertical cylinder with variable temperature and mass diffusion. Casson fluid flow past on vertical cylinder in the presence of chemical reaction and magnetic field was analysed by Kumar and Rizvi [4].

Dufour and Soret effects on unsteady MHD convective heat and mass transfer flow due to a rotating disk was studied by Maleque [5]. Alam and Rahman [7] has worked on Dufour and soret effects on MHD free convective heat and mass transfer flow past a vertical porous flat plate embedded in a porous medium and the equations of the model are solved numerically by using the Nachtsheim-Swigert shooting method. They noticed that Large Darcy number leads to the increase of the velocity and decrease of the temperature as well as concentration of the fluid increase within the boundary layer. Jain and Bohra [8] worked on Soret and Dufour effects on radiative free convection flow and mass transfer over a sphere with velocity slip and thermal jump. Hayat et al. [9] worked on numerical simulation for nonlinear radiative flow by convective cylinder and found that the flow velocity decreases and temperature increases when magnetic parameter is enhanced. Unsteady MHD free convection oscillatory Couette flow through a porous medium with periodic wall temperature in presence of chemical reaction and thermal radiation was studied by Reddy et al. [10]. They have used to analytically method to solve the coupled non-linear governing

equations and found that chemical reaction parameter increases the fluid velocity while decreased the concentration level of the fluid. Abbas et al. [11] has presented fluid model on heat transfer analysis due to an unsteady stretching/shrinking cylinder with partial slip condition and suction. They have solved flow model numerically by using Runge-Kutta-Fehlberg method. Unsteady MHD flow through porous medium past an exponentially accelerated inclined cylinder with variable oscillating wall temperature in the presence of chemical reaction was studied by us [6]. The flow model under consideration analyzes the combined effects of Soret and Dufour on unsteady MHD flow past through inclined cylinder with variable oscillating wall temperature. The problem of the flow model is solved by numerically using Crank-Nicolson implicit finite-difference technique.

2. Mathematical Analysis

In this paper, consider unsteady MHD flow of an incompressible, viscous, electrically conducting fluid mixture past through a moving inclined cylinder of radius r_0. Here the x-axis is taken along the axis. The cylinder is inclined at an angle φ from vertical plane and the radial coordinate r is taken normal to the cylinder. The gravitational acceleration g is acting downward. The magnetic field B_0 of uniform strength is applied perpendicular to the flow. During the motion, the direction of the magnetic field changes along with the plate in such a way that it always remains perpendicular to it. This means, the direction of magnetic field is tied with the plate. Initially it has been considered that the plate as well as the fluid is at the same temperature T_∞. The species concentration in the fluid is taken as C_∞ for all $t \le 0$. At time $t > 0$, the cylinder starts exponentially accelerated with acceleration parameter b and temperature of the Wall T_w is oscillating with phase angle ωt. The concentration C_w near the surface is raised linearly with respect to time. Then under these assumptions and the Boussinesq's approximation, the flow is governed by the following system of equations:

$$\frac{\partial u}{\partial t} = \upsilon \frac{\partial^2 u}{\partial r^2} + \frac{\upsilon}{r}\frac{\partial u}{\partial r} + g\beta (T - T_\infty) Cos\phi + g\beta^* (C - C_\infty)\cos\phi$$

$$-\frac{\sigma B_0^2 u}{\rho}-\frac{\upsilon u}{K} \tag{1}$$

$$\frac{\partial T}{\partial t}=\alpha\frac{\partial^2 T}{\partial r^2}+\frac{\alpha}{r}\frac{\partial T}{\partial r}+\frac{D_m K_T}{C_s C_p}\frac{\partial^2 C}{\partial r^2} \tag{2}$$

$$\frac{\partial C}{\partial t}=D\frac{\partial^2 C}{\partial r^2}+\frac{D}{r}\frac{\partial C}{\partial r}+\frac{D_m K_T}{T_m}\frac{\partial^2 T}{\partial r^2} \tag{3}$$

Initial and boundary conditions are as follows:

$$\left.\begin{aligned} &t\le 0: u=0, T=T_\infty, C=C_\infty, \text{for every} r\\ &t>0: u=u_0, T=T_\infty+(T_w-T_\infty)Cos\omega o, C=C_\infty+(C_w-C_\infty)\frac{tv}{r_0^2}, \text{ at } r=r_0\\ &u\to 0, T\to T_\infty, C\to C_\infty \text{ as } r\to\infty \end{aligned}\right\} \tag{4}$$

Here u is the velocity of fluid, g-the acceleration due to gravity, β-volumetric coefficient of thermal expansion, t-time, T-temperature of the fluid, β^*-volumetric coefficient of concentration expansion, C-species concentration in the fluid, ν-the kinematic viscosity, ρ-the density, C_p-the specific heat at constant pressure, k-thermal conductivity of the fluid, D-the mass diffusion coefficient, T_w-temperature of the plate at $z = 0$, C_w-species concentration at the plate $z = 0$, B_0-the uniform magnetic field, K-the permeability parameter, K_c-chemical reaction, σ-electrical conductivity.

Equations (1), (2), and (3) are converted to dimensionless form by the following non-dimensional quantities:

$$\left.\begin{aligned} &R=\frac{r}{r_0}, \bar{u}=\frac{u}{u_0}, \theta=\frac{(T-T_\infty)}{(T_w-T_\infty)}, S_c=\frac{v}{D}, \mu=\rho v, \bar{\omega}=\frac{\omega v}{u_0^2}, \bar{C}=\frac{(C-C_\infty)}{(C_w-C_\infty)},\\ &P_r=\frac{v}{a}, G_r=\frac{g\beta\beta v(T_w-T_\infty)}{u_0^3}, M=\frac{\sigma B_0^2 r_0^2}{v\rho}, \ D_f=\frac{D_m K_T T_\infty (C_w-C_\infty)}{v C_s C_p (T_w-T_\infty)},\\ &G_m=\frac{g\beta^* v(C_w-C_\infty)}{u_0^3}, \bar{K}=\frac{u_0}{v^2}K, \ S_r=\frac{D_m K_T T_\infty}{v T_m (C_w-C_\infty)}, \ \bar{t}=\frac{tv}{r_0^2} \end{aligned}\right\} \tag{5}$$

where $\bar{u}$ is the dimensionless Primary velocity, $\bar{v}$-the secondary velocity, $\bar{b}$-dimensionless acceleration parameter, $\bar{t}$-dimensionless time, θ-the

dimensionless temperature, $\overline{C}$ -the dimensionless concentration, G_r -thermal Grashof number, G_m -mass Grashof number, μ-the coefficient of viscosity, $\overline{K}$ -the dimensionless permeability parameter, K_0 -chemical reaction parameter, P_r -the Prandtl number, S_c -the Schmidt number, D_f -Dofour number, S_r -Soret number M-the magnetic parameter.

The flow model is as follows in dimensionless form:

$$\frac{\partial \overline{u}}{\partial \overline{t}} = \frac{\partial^2 \overline{u}}{\partial R^2} + \frac{1}{R}\frac{\partial \overline{u}}{\partial R} + G_r \theta Cos\varphi + G_m\, \overline{C} Cos\varphi - M\overline{u} - \frac{1}{\overline{K}}\overline{u} \tag{6}$$

$$\frac{\partial \theta}{\partial \overline{t}} = \frac{1}{P_r}\frac{\partial^2 \theta}{\partial R^2} + \frac{1}{R\,P_r}\frac{\partial \theta}{\partial R} + D_f \frac{\partial^2 C}{\partial R^2} \tag{7}$$

$$\frac{\partial \overline{C}}{\partial \overline{t}} = \frac{1}{S_c}\frac{\partial^2 \overline{C}}{\partial R^2} + \frac{1}{R\,S_c}\frac{\partial \overline{C}}{\partial R} + S_r \frac{\partial^2 \theta}{\partial R^2} \tag{8}$$

The boundary conditions (4) that result are as follows:

$$\left.\begin{array}{c} \overline{t} \le 0 : \overline{u} = 0,\ \theta = 0,\ \overline{C} = 0, \text{ for every R} \\ \overline{t} > 0 : \overline{u} = 1,\ \theta = Cos\overline{\omega}\overline{t},\ \overline{C} = \overline{t}, \text{ at } R = 0 \\ \overline{u} \to 0,\ \theta \to 0,\ \overline{C} \to 0, \text{ as } R \to \infty \end{array}\right\} \tag{9}$$

By removing bars from the equations above, we obtain

$$\frac{\partial u}{\partial t} = \frac{\partial^2 u}{\partial R^2} + \frac{1}{R}\frac{\partial u}{\partial R} + G_r \theta Cos\phi + G_m C Cos\phi - Mu - \frac{1}{K}u \tag{10}$$

$$\frac{\partial \theta}{\partial t} = \frac{1}{P_r}\frac{\partial^2 \theta}{\partial R^2} + \frac{1}{R\,P_r}\frac{\partial \theta}{\partial R} + D_f \frac{\partial^2 C}{\partial R^2} \tag{11}$$

$$\frac{\partial C}{\partial t} = \frac{1}{S_c}\frac{\partial^2 C}{\partial R^2} + \frac{1}{R\,S_c}\frac{\partial C}{\partial R} + S_r \frac{\partial^2 \theta}{\partial R^2} \tag{12}$$

The boundary conditions become

$$\left.\begin{array}{c} t \le 0 : u = 0,\ \theta = 0,\ C = 0, \text{ for every R} \\ t > 0 : u = 1,\ \theta = Cos\omega t,\ C = t, \text{ at } R = 0 \\ u \to 0,\ \theta \to 0,\ C \to 0, \text{ as } R \to \infty \end{array}\right\} \tag{13}$$

3. Method of Solution

Boundary and initial conditions (13) are used to solve the nonlinear partial differential equations (10) to (12). The Crank-Nicolson implicit finite difference method is used to numerically solve these non-linear partial differential equations. The following are the finite difference equations that relate to equations (10) to (12):

$$u_i^{j+1} - u_i^j = \frac{\Delta t}{2(\Delta R)^2}(u_{i+1}^j - 2u_i^j + u_{i-1}^j + u_{i+1}^{j+1} - 2u_i^{j+1} + u_{i-1}^{j+1})$$

$$+ \frac{\Delta t}{4(1+(i-1)\Delta R)(\Delta R)}(u_{i+1}^j - u_{i-1}^j + u_{i+1}^{j+1} - u_{i-1}^{j+1})$$

$$+ \frac{\Delta t G_r Cos\phi}{2}((\theta_i^{j+1} + \theta_i^j)) + \frac{\Delta t G_m Cos\phi}{2}(C_i^{j+1} + C_i^j) - \frac{\Delta t}{2}(M + \frac{1}{K})(u_i^{j+1} + u_i^j) \tag{14}$$

$$\theta_i^{j+1} - \theta_i^j = \frac{\Delta t}{2P_r(\Delta R)^2}(\theta_{i+1}^j - 2\theta_i^j + \theta_{i-1}^j + \theta_{i+1}^{j+1} - 2\theta_i^{j+1} + \theta_{i-1}^{j+1})$$

$$+ \frac{\Delta t}{4P_r\,(1+(i-1)\Delta R)(\Delta R)}(\theta_{i+1}^j - \theta_{i-1}^j + \theta_{i+1}^{j+1} - \theta_{i-1}^{j+1})$$

$$+ D_f \frac{\Delta t}{2(\Delta R)^2}(C_{i+1}^j - 2C_i^j + C_{i-1}^j + C_{i+1}^{j+1} - 2C_i^{j+1} + C_{i-1}^{j+1}) \tag{15}$$

$$C_i^{j+1} - C_i^j = \frac{\Delta t}{2S_c(\Delta R)^2}(C_{i+1}^j - 2C_i^j + C_{i-1}^j + C_{i+1}^{j+1} - 2C_i^{j+1} + C_{i-1}^{j+1})$$

$$+ \frac{\Delta t}{4S_c(1+(i-1)\Delta R)(\Delta R)}(C_{i+1}^j - C_{i-1}^j + C_{i+1}^{j+1} - C_{i-1}^{j+1})$$

$$+ \frac{S_r \Delta t}{2(\Delta R)^2}(\theta_{i+1}^j - 2\theta_i^j + \theta_{i-1}^j + \theta_{i+1}^{j+1} - 2\theta_i^{j+1} + \theta_{i-1}^{j+1}) \tag{16}$$

In the above solution, the index i refers to R and j refers to time t, $\Delta t = t_{j+1} - t_j$ and $\Delta R = R_{j+1} - R_j$. For calculating the values of u, θ and C at time t, it compute the values at time $t + \Delta t$ as follows: here, substitute

$i = 1, 2, \ldots, N-1,$ as N is corresponded to ∞. The implicit Crank-Nicolson finite difference method is a second order method $(o(\Delta t^2))$ in time and has no restriction on space and time steps, that is, the method is unconditionally stable. The computation is executed for $\Delta R = 0.1$, $\Delta t = 0.002$ and procedure is repeated till $R = 40$.

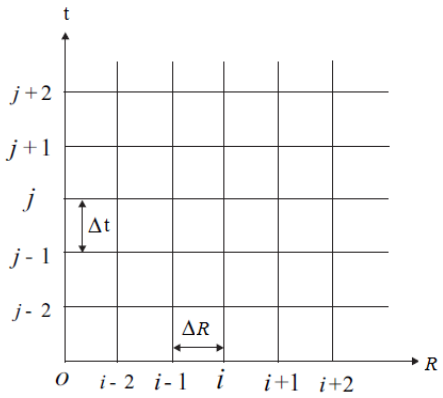

Figure A. Finite Difference grids.

The implicit method provides solutions for the stable fluid model. Matrix inversions are called for by this procedure, which we were already done in a prior step. This problem has to do with initial-boundary values for spatial grids with a finite number of points.

As a result, the relevant flow model equations may not always guarantee mesh convergence. In order to optimise numerical efficiency, we used the tridiagonal technique to solve the two-point conditions governing the primary connected governing system equations of momentum, energy, and diffusion. The method's numerical stability is guaranteed by the implicit nature of the numerical approach, and the process's convergence (consistency) is quite satisfactory. Therefore, the strategy makes sense. Consistency and stability ensure convergence.

4. Stability Analysis of the Solution

The stability criterion of the finite difference scheme for constant mesh sizes are analyzed by using Von-Neumann Technique. This method was

explained by Carnahan et al. (1969). In the Fourier expansion, the general term for u, θ, C at a time arbitrarily called $t = 0$, are assumed to be of the form $e^{i\beta R}$ where $i = \sqrt{-1}$. At a later time, these terms will become,

$$u = \eta(t)e^{i\beta R}, \tag{17}$$

$$\theta = H(t)\,e^{i\beta R}, \tag{18}$$

$$C = \xi(t)\,e^{i\beta R}. \tag{19}$$

Putting the values of equations (17) to (19) in equations (14) to (16) under the assumption that the coefficients u, θ, C as constants over any one time step and denoting the values after one time step by η', H' and ξ'. After simplification, we have

$$\frac{\eta'-\eta}{\Delta t} = \frac{G_r(H'+H)Cos\phi + G_m(\xi'-\xi)Cos\phi}{2} + \frac{\{\cos(\beta\Delta R)-1\}}{(\Delta R)^2}(\eta'+\eta)$$

$$-\frac{1}{2}\left(M + \frac{1}{K}\right)(\eta'+\eta) + \frac{i\sin(\beta\Delta R)}{2\Delta R(1+(i-1)\Delta R)}(\eta'+\eta), \tag{20}$$

$$\frac{H'-H}{\Delta t} = \frac{(H'+H)}{\Pr}\left[\frac{\cos(\beta\Delta R)-1}{(\Delta R)^2} + \frac{i\sin(\beta\Delta R)}{2\Delta R(1+(i-1)\Delta R)}\right]$$

$$+ D_f\,\frac{(\xi'+\xi)}{(\Delta R)^2}(\cos(\beta\Delta R)-1), \tag{21}$$

$$\frac{\xi'-\xi}{\Delta t} = \frac{(\xi'+\xi)}{Sc}\left[\frac{\cos(\beta\Delta R)-1}{(\Delta R)^2} + \frac{i\sin(\beta\Delta R)}{2\Delta R(1+(i-1)\Delta R)}\right]$$

$$+ S_r\,\frac{(H'+H)}{(\Delta R)^2}(\cos(\beta\Delta R)-1) \tag{22}$$

Equations (20) to (22) can be rewritten as,

$$(1+A)\eta' = (1-A)\eta + \frac{G_r}{2}(H'+H) + \frac{G_m}{2}(\xi'+\xi), \tag{23}$$

$$(1+G)H' = (1-G)H + D_f \frac{(\xi'+\xi)}{(\Delta R)^2}(\cos(\beta\Delta R)-1), \tag{24}$$

$$(1+E)\xi' = (1-E)\xi + S_r \frac{(H'+H)}{(\Delta R)^2}(\cos(\beta\Delta R)-1), \tag{25}$$

where,

$$A = \frac{\{1-\cos(\beta\Delta R)\}(\Delta t)}{(\Delta R)^2} + \frac{(\Delta t)}{2}\left(M + \frac{1}{K}\right) - \frac{(\Delta t)\, i \sin(\beta\Delta R)}{2\Delta R(1+(i-1)\Delta R)},$$

$$G = \frac{\{1-\cos(\beta\Delta R)\}(\Delta t)}{P_r(\Delta R)^2} - \frac{(\Delta t)\, i \sin(\beta\Delta R)}{2P_r\Delta R(1+(i-1)\Delta R)},$$

$$E = \frac{\{1-\cos(\beta\Delta R)\}(\Delta t)}{S_c(\Delta R)^2} - \frac{(\Delta t)\, i \sin(\beta\Delta R)}{2S_c\Delta R(1+(i-1)\Delta R)}$$

$$a = \frac{(\cos(\beta\Delta R)-1)}{(\Delta R)^2}\Delta t.$$

Eliminating H' and ξ' in equation (23) by using (24) and (25). The resultant equation is of the form,

$$\eta' = A_1\eta + A_2 H + A_3\xi. \tag{26}$$

$$H' = A_4 H + A_5\xi. \tag{27}$$

$$\eta' = A_6 H + A_7\xi. \tag{28}$$

Equations (26) to (28) can be written in matrix form as,

$$\begin{pmatrix} \eta' \\ H' \\ \xi' \end{pmatrix} = \begin{pmatrix} A_1 & A_2 & A_3 \\ 0 & A_4 & A_5 \\ 0 & A_6 & A_7 \end{pmatrix} \begin{pmatrix} \eta \\ H \\ \xi \end{pmatrix}. \tag{29}$$

In above matrix, $A_1 = \frac{(1-A)}{(1+A)}$, $A_2 = \frac{G_r}{b(1+A)} + \frac{G_m a \cdot S_r}{b(1+E)(1+A)}$

$$A_3 = \frac{G_r D_f a}{b(1+A)(1+E)} + \frac{G_m}{(1+E)(1+A)} + \frac{G_m D_f a \cdot S_r}{b(1+E)^2(1+A)},$$

$$A_4 = \left((1-G)+\frac{D_f S_r a^2}{((1+E))}\right) \Big/ \left((1-G)-\frac{D_f S_r a^2}{((1+E))}\right),$$

$$A_5 = \left(\frac{2D_f a^2}{((1+E))}\right) \Big/ \left((1-G)-\frac{D_f S_r a^2}{((1+E))}\right),$$

$$A_6 = \frac{2a \cdot S_r}{b(1+E)},$$

$$A_7 = \frac{(1-E)}{(1+E)} + \frac{2D_f a^2 S_r}{b(1+E)^2}.$$

For obtaining the stability condition regarding this explicit finite difference solution, the dimensionless time difference Δt is very small i.e. tends to zero. Under this condition, $A_5 \to 0$ and $A_6 \to 0$. According stability analysis of the finite difference scheme, the modulus of each Eigen value of the amplification matrix does not exceed unity. Since the matrix equation (27) in triangular form, the Eigen values are its diagonal elements. Therefore, the Eigen values of the amplification matrix are $\lambda_1 = A_1 \lambda_2 = A_4 \lambda_3 = A_7$. Since the real part of F is greater than or equal to zero, thus $|A_1| \le 1$ similarly, $|A_4| \le 1$ and $|A_7| \le 1$. Hence, the finite difference scheme is unconditionally stable. The Crank-Nicolson scheme has a truncation error of $O(\Delta t^2 + \Delta R^2)$, i.e. the temporal truncation error is significantly small. It tends to zero as Δt and ΔR tend to zero. So, the scheme is compatible. Stability and compatibility ensures convergence.

5. Results and Discussion

In this paper, the numerically results were obtained and these results shown graphically with the help of following figures. Figures 1 to 8 illustrate the study of flow behavior of MHD fluid for various parameters, including the thermal Grashof number (Gr), mass Grashof number (Gm), angle of inclination of surface (ϕ), permeability parameter (K), angular frequency (ω_e), magnetic field parameter (M), Dufour number (D_f), Soret number

(S_r). Figure 1 shows that the velocities increase throughout the boundary layer region as the mass Grashof number Gm increases. Figure 2 shows that speeds grow as the thermal Grashof number Gr. This indicates that the MHD flow is accelerated as a result of an increase in buoyant force caused by a rise in the thermal Grashof number. The positive values of Gr indicate that the cylinder's surface has cooled via free convection. As a result, heat is transferred from the vertical cylinder into the fluid, raising its temperature and boosting the buoyant force. Additionally, it can be observed that when the thermal Grashof number rises, the peak values of the velocity grow fast close to the surface and then slowly decelerate to the free stream velocity. In light of this, it may be said that buoyancy force tends to increase fluid velocity close to the surface. Figure 3 demonstrates the fluid's velocity drops as the plate angle ($\emptyset$) rises. The fluid's velocity decreases as the surface slopes away from vertical, which is consistent with the actual flow. The influence of the Dufour number is shown in Figure 4. It is obvious that the velocity distribution in the boundary layer increases as the Dufour number increases. Furthermore, we see that the velocity increases with an increase in the permeability parameter K (figure 5), which is obvious given that an increase in porosity of the medium. As a result, the resistance of the porous medium reduces as the porosity parameter K increases, which tends to speed up the flow. It is observed from figure 6 that the effect of increasing values of the parameter M results in decreasing the fluid velocity. It is due to the application of transverse magnetic field that acts as Lorentz's force which retards the flow. Figure 7 depicts the influence of the Soret number at various points in time. It can be seen that when the Soret number rises, the velocity also increases. It is noticed that the velocity decreases as the angular frequency is increased (figure 8).

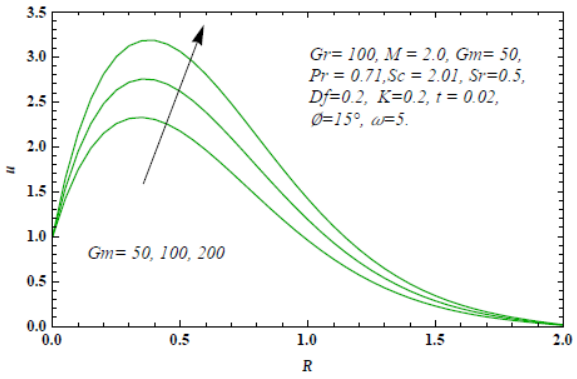

Figure 1. Velocity u for different values of Gm

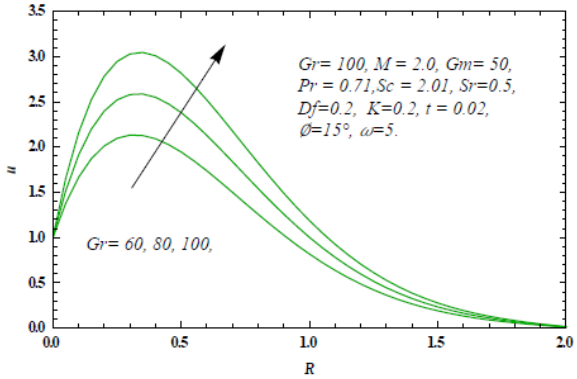

Figure 2. Velocity u for different values of Gr

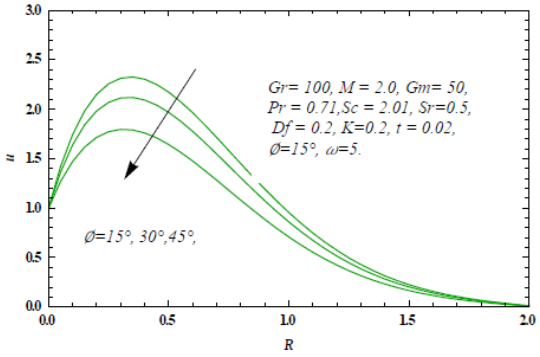

Figure 3. Velocity u for different values of φ

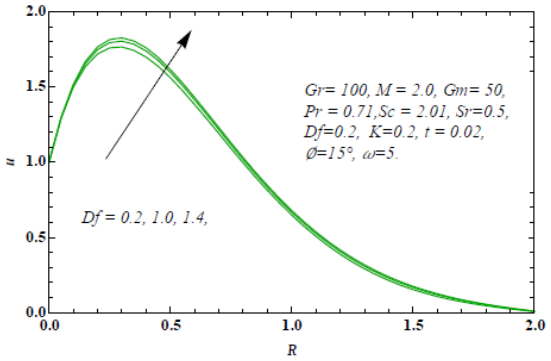

Figure 4. Velocity u for different values of D_f

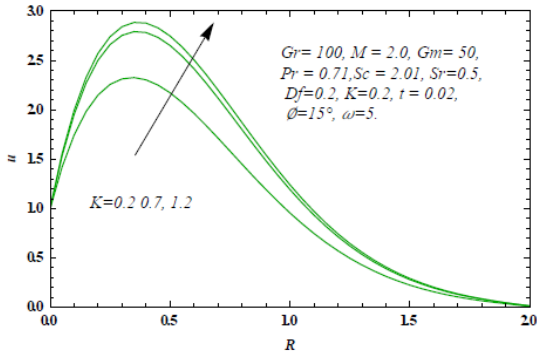

Figure 5. Velocity u for different values of K

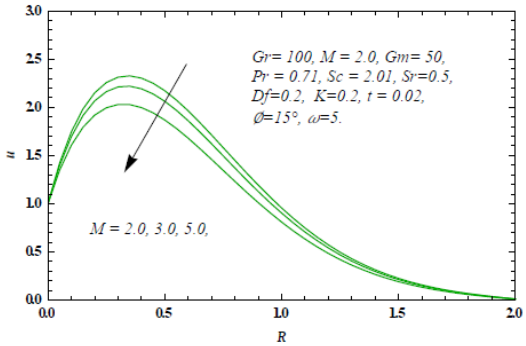

Figure 6. Velocity u for different values of M

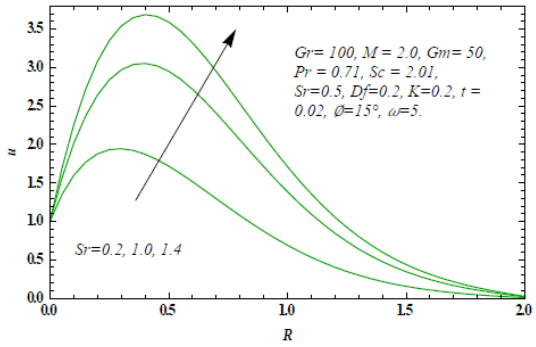

Figure 7. Velocity u for different values of S_r

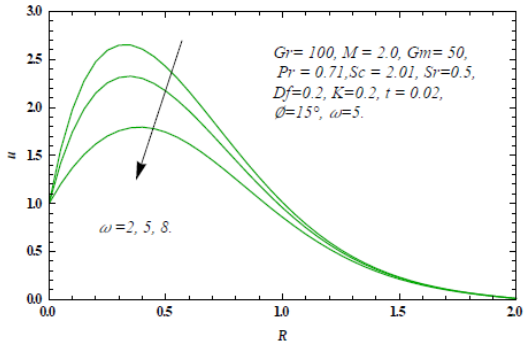

Figure 8. Velocity u for different values of ω.

6. Conclusion

The numerical analysis for the model under discussion, the governing non-linear partial differential equations were transformed into non-dimensional form. Equations for motion, diffusion, and energy make up the model. Standard sets of the parameter values have been taken in order to investigate the solutions found. We found that when the values of the permeability parameter, Soret, Dufour, and Grashof numbers, porosity of the medium is increased then the fluid's velocity increases. While the other parameters like surface's angle, angular frequency and the magnetic field parameter, the pattern is reversed. The MHD flow model's solution is unconditionally stable and Convergence is guaranteed by compatibility with stability. We discovered that the numerical results match the actual flow characteristics of MHD fluid.

References

[1] Abid Majeed, Tariq Javed and Irfan Mustafa, Heat transfer analysis of boundary layer flow over hyperbolic stretching cylinder, Alexandria Engineering Journal 55 (2016), 1333-1339.

[2] D. Srinivasacharya B. Mallikarjuna and R. Bhuvanavijaya, Soret and Dufour effects on mixed convection along a vertical wavy surface in a porous medium with variable properties, Ain Shams Engineering Journal 6 (2015), 553-564.

[3] G. Kumar, A. Kumar, M. K. Misra and V. Srivastava, Chemical reaction effect on MHD flow past an impulsively started vertical cylinder with variable temperature and mass diffusion, Journal of Science and Arts 47(2) (2019), 513-522.

[4] Gaurav Kumar and S. M. K. Rizvi, Casson fluid flow past on vertical cylinder in the presence of chemical reaction and magnetic field 169(1) (2021), 524-537.

[5] Kh. A. Maleque, Dufour and Soret effects on unsteady MHD convective heat and mass transfer flow due to a rotating disk Lat. Am. appl. res. 40(2) (2010).

[6] M. Kumar, G. Kumar and A. W. Khan, unsteady MHD flow through porous medium past an exponentially accelerated inclined cylinder with variable oscillating wall temperature in the presence of chemical reaction, GANITA 72(2) (2022), 103-113.

[7] Md. Shariful Alam and Mohammad Mansur Rahman, Dufour and Soret effects on MHD free convective heat and mass transfer flow past a vertical porous flat plate embedded in a porous medium Journal of Naval Architecture and Marine Engineering June 1 (2005), 55-65.

[8] Shalini Jain and Shweta Bohra, Soret/Dufour effects on radiative free convection flow and mass transfer over a sphere with velocity slip and thermal jump, Walailak Journal of Science and Technology (WJST) 16(9) (2019), 701-721.

[9] Tasawar Hayat, Muhammad Tamoor, Muhammad Ijaz Khan and Ahmad Alsaedi, Numerical simulation for nonlinear radiative flow by convective cylinder, Results in Physics 6 (2016), 1031-1035.

[10] T. Sudhakar Reddy, M. C. Raju and S. V. K. Varma, Unsteady MHD free convection oscilatory couette flow through a porous medium with periodic wall temperature in presence of chemical reaction and thermal radiation, International Journal of Science and Advanced Technology 1(10) (2011), 51-58.

[11] Z. Abbas, S. Rasool and M. M. Rashidi, Heat transfer analysis due to an unsteady stretching/shrinking cylinder with partial slip condition and suction, Ain Shams Engineering Journal 6 (2015), 939-945.